Effect of DFIG Wind Farm Fault Currents on the Transformer Differential Relaying Performance

Huy Nguyen-Duc, *IEEE member*
Department of Electric power systems,
Hanoi University of Science and Technology
Hanoi, Vietnam

Yosuke Nakanishi
Graduate School of Energy and Environment
Waseda University
Tokyo, Japan

***Abstract*—Nowadays, the wind energy is one of the fastest growing renewable energies in the world. The increasing presence of wind farms with electronic controls pose several issues for the protective relaying systems. The issues with conventional protection relays when applied to wind farm protection is due to the fact that short circuit currents from wind farm, especially those based on type III and type IV, are fundamentally different from short-circuit currents of synchronous generators. This paper investigates the performance of a typical differential protection scheme for a 110kV power transformer which connects a DFIG wind farm to the grid. The simulation results show that wind farm short circuit current might cause incorrect relay operation.**

***Index Terms*--power system relaying, wind power, short-circuit current.**

I. INTRODUCTION

With the depletion of fossil fuel sources, the growing development of renewable energy sources is necessary. Among renewable energy sources, the wind farms have become more and more integrated into the power systems. However, the increasing penetration level of wind energy also pose several technical challenges. Wind farm generators are not designed based on conventional synchronous machines. Instead, most wind farms nowadays are based on Doubly Fed Induction Machines and Fully rated Converters. These new types of wind farm use electronic based system to control the active and reactive power flows. This brings forward the following technical issues:

- Since high power rating inverters are present in the wind farms (especially those based on type IV), the control systems in the wind farm respond very quickly. It has been observed that wind farms do not take part in the system's inertia, unlike conventional synchronous machines. Hence, it is expected that systems with high wind penetration might experience larger frequency deviations following system disturbances.
- As the active/reactive power of wind farms are controlled by high speed electronic circuits, the short-circuit current characteristic of wind farms is also fundamentally different to that of synchronous machines. Recent reports have shown that wind farm short circuit currents may contain large amount of DC current [1-2]. The short circuit current behavior is further complicated by the fact that several other control schemes also come into play during voltage dip events, such as the LVRT controllers. It should be noted that the characteristic of LVRT controller may vary considerably among different vendors and is also influenced by grid codes.

With the above reasons, the presence of wind farms have raised issues relating to secure operation, maintaining reliability of supply, relay coordination, etc. Regarding protective relaying system, a lot of effort has been made to analyze the fault current characteristic from wind farms. The results have been reported in recent publications from the Power system Relaying Committee [1]. Overall, the fault current characteristic of type III and type IV wind farms vary considerably, depending on the fault severity, as well as the control strategies implemented in the wind farm control system for LVRT requirement, etc. In [3], the performance of line differential protection as affected by DFIG wind farm has been studied. It is shown that under the influence of wind farm control system, the sensitivity might be insufficient, and the fault selection logic might not perform correctly in some cases. Reference [4] shows that DFIG fault current may cause mal-operation of the current differential protection scheme.

This paper investigates the fault current characteristic of wind farms based on Doubly Fed Induction Generator (DFIG) technology. It is observed that the fault current from wind farms can contain large DC offset and a larger amount of harmonics, the current transformer for protective relaying purpose may not function accurately. Therefore, the detailed model of current transformer with saturation effect is considered in this study.

The paper is organized as follows: Section II introduces principles of DFIG operation and its simulation models. Section III presents the simulation model for the differential relaying scheme. The simulation results are shown in section IV. The discussions and conclusion are given in section V.

978-1-5386-4291-7/18/$31.00 ©2018 IEEE

II. DOUBLY FED INDUCTION GENERATOR

A. Principle of operation

The basic structure of a DFIG (type III) wind generator is shown in Fig. 1. It consists of an induction generator, where the stator side is directly connected to the grid. The rotor side is connected to the grid via a back-to-back converter. When the induction machine speed is below the synchronous speed, the back-to-back converter receives active power from the grid; if the machine speed is above the synchronous speed, then active power from the rotor is transferred to the grid via the back-to-back converter.

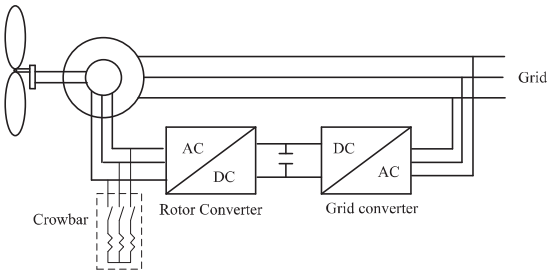

Figure 1 Structure of a Doubly Fed Induction generator.

The operation of a DFIG is ensured by three control loops as follows [5]:

- The turbine controller: The main objective of the turbine controller is to change the speed set point of the turbine, so that maximum power can be received from wind energy. Based on current wind speed, the optimal tip to speed ratio can be determined. The turbine controller also provides a reference electromagnetic torque signal to the rotor-side converter.
- The Rotor-side Converter controller (RSC): The main control function of the RSC controller is to regulate the electromagnetic torque, as specified by the turbine control. The structure of the RSC controller is shown in Fig.2.
- The Grid-side Converter controller (GSC): The GSC controller regulates the DC link voltage. Besides, it can be used to regulate the reactive power injecting to the grid. The basic structure of the GSC controller is shown in Fig.3.

B. DFIG simulation models

The complete model of the DFIG comprises a large number of elements. There are several simulation models for the DFIG, depending on the specific application and level of accuracy required. The r.m.s model is the simplest form of Doubly Fed Induction Generator. In this model, the dynamics of the internal electronic control system of the DFIG is ignored, because it is considered very fast, compared to the power system electromechanical dynamics. This model is often suitable for grid impact study [6].

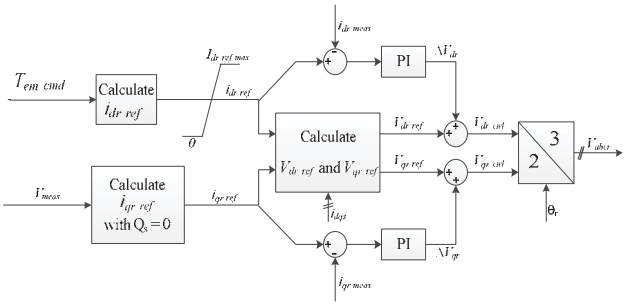

Figure 2 The RSC controller.

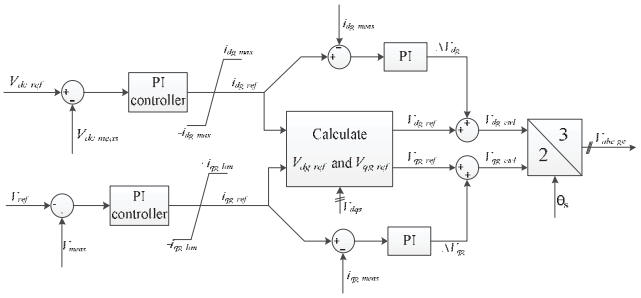

Figure 3 The GSC controller.

For the analysis of protective relay performance, the r.m.s model does not however provide appropriate accuracy [1]. In order to evaluate the performance of high speed relay schemes, such as those based on differential and distance protection, a detailed electromagnetic transient model of the wind generator and its control system need to be used. This model represents in detail the rotor-side, grid-side control system, as well as the dynamics of PWM controls, and various protection and control strategies during grid faults.

C. Crowbar protection

To prevent the wind generator from excessive over-voltage due to short-circuit, a special crowbar circuit is used. When activated, the crowbar limit the voltage on the rotor. But it also affects the fault current waveform. Parameters of crowbar protection schemes, such as the crowbar resistance, time delay, etc. have been shown to strongly affect the fault current behavior off DFIG based wind farm.

III. MODELING OF DIFFERENTIAL RELAYS

This section presents the simulation model for the differential relaying scheme. For protecting power transformers, the differential protection scheme is often chosen, because of its selectivity and reliability. The basic principle of differential protection as applied to power transformer protection is depicted in Fig. 4.

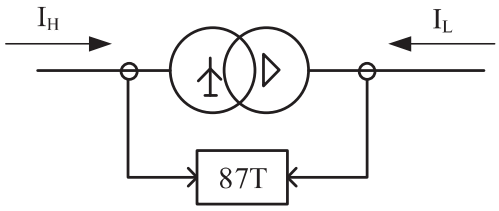

Figure 4 Principle of differential protection for power transformer.

The power transformer differential protection (ANSI code 87) operates based on two quantities, namely the differential current and the stabilizing current, which are calculated as follows:

$$I_{DIFF} = |K_H I_H + K_L I_L| \quad (1)$$

$$I_{STAB} = |K_H I_H| + |K_L I_L| \quad (2)$$

where $I_H = [I_H^A, I_H^B, I_H^C]^T$ is the vector of high-side currents, $I_L = [I_L^A, I_L^B, I_L^C]^T$ is the vector of low side currents; K_H and K_L are the transformation matrices which depend on the transformer vector group. A typical operating characteristic of the transformer differential protection is shown in the Fig. 5. In normal operating condition, the tripping threshold is determined by section a. When the fault current is high, the threshold is increased according to the stabilization current (sections b and c).

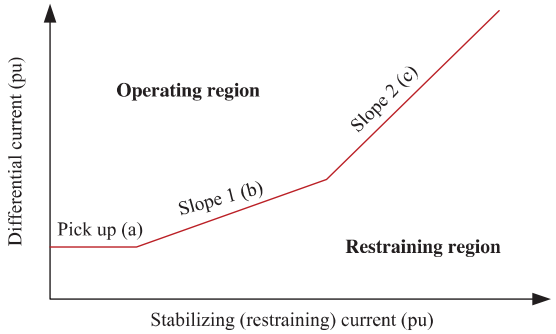

Figure 5 Operating characteristic of transformer differential protection.

To ensure correct operation of transformer differential protection under current transformer (CT) saturation, additional add-on stabilization can be used. Besides, digital transformer differential protection also provides blocking function upon detection of inrush currents.

The performance of transformer differential protection is highly affected by the accuracy of current transformer. For power system with high X/R ratio, and when there is heavy DC offset in the fault current, the CT may experience severe saturation during through fault and may trigger incorrect operation of the differential protection [7]. Therefore, it is very necessary to represent accurately the model of CT in the analysis of differential protection.

In this work, the CT model is constructed based on excitation curves of actual current transformers. The V-A characteristic of several different protection class CTs are collected. We follow the instructions in [8] to develop a simulation model for the current transformer in the Simulink/Simpowersystem toolbox, based on its measured V-A characteristic.

IV. SIMULATION RESULTS

The power system model simulated in this work is shown in Fig. 7. It consists of a 110kV grid which is connected to the national grid, as well as a wind farm. The performance of the transformer differential relay is evaluated, under different fault scenarios.

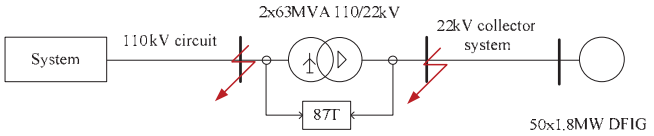

Figure 6 Simulation model.

The simulation model is developed using MATLAB/Simpowersystem toolbox. The wind generator is modeled using highly detailed model, including the PWM control of the rotor side and grid side converters. Besides, the wind generators are equipped with crowbar control and current limiter control. The two main faults considered in the simulations are at 110kV and 22kV bus. These are considered external faults for the transformer differential protection, for which it is not supposed to trip.

A. Wind farm fault current

Fig. 7 shows the simulation results when a 3-phase fault is applied at the high side of the 110kV power transformer. The fault is applied at 0.1s and is cleared at 0.2s. During the fault, the DC link voltage increases sharply, until the crowbar control circuit activates. When the crowbar control is not activated, the fault current from the wind farm, for the same fault is shown in Fig. 8. Without crowbar action, the DC link overvoltage is very high. These short circuit current waveforms are quite similar to those reported in [1-2].

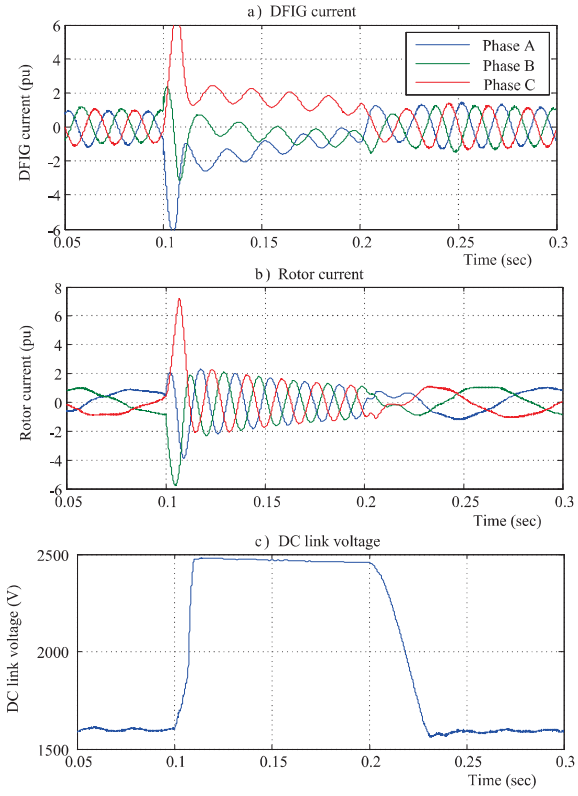

Figure 7 Wind farm short circuit currents and DC link voltage, with 3 phase fault at high side bus.

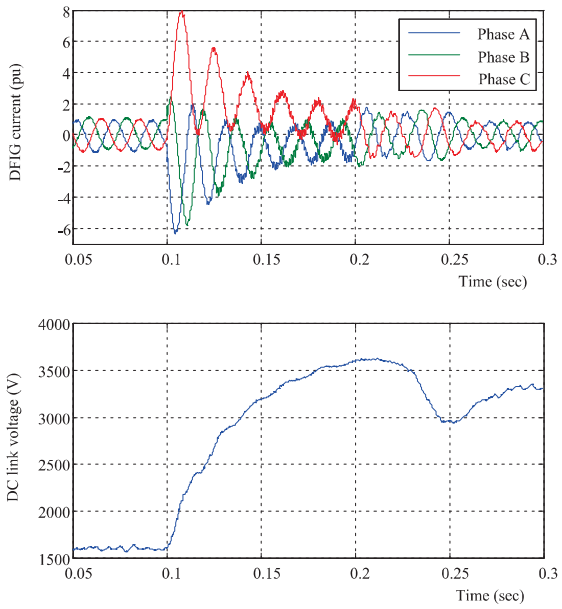

Figure 8 DFIG fault current without crowbar.

B. *Performance of transformer differential protection*

To examine the performance of the transformer differential protection system, we use typical transformer differential protection setting from SIEMENS relays [7], as follows:

- Branch a: Idiff> = 0.3 pu
- Branch b: SLOPE = 25%
- Branch c: SLOPE = 50%, base point = 2.5pu.

One of the reason for mal-operation of the transformer differential protection is the saturation of its core. The saturation can be caused by high inrush current upon transformer energization, sympathetic inrush, or by the fault clearing current [10]. The simulated differential and stabilizing currents, with and without consideration of transformer saturable core are shown in Fig. 9. Note that the saturation model of the current transformers, with secondary burden of 2Ω is also included in the simulation. The simulations are also carried out with different models of current transformer (varying secondary burdens and excitation curve characteristics), however the change in CT model does not result in substantial difference in the simulated differential and stabilizing currents. On the other hand, the results shows that in case the transformer saturable core is considered, there is a surge in the differential current at the moment when the fault is cleared. After the fault is cleared at t = 0.2s, the increase in differential current is due to the transients when GSC and RSC resume normal operation. This transient current causes asimilar effect to that of the inrush current, which saturates the transformer core.

Fig. 10 shows the operation of differential protection element, with 3-phase fault and 2-phase-to-ground fault at the 110kV bus. After the fault is applied at t = 0.1s, the stabilizing current reaches highest value at t = 0.11s, then decreases. After the fault is cleared at t = 0.2s, the crowbar is deactivated, and the rotor-side controller resumes operation. Due to the surge in differential current after the fault is cleared, the operating point of the differential protection briefly entered the tripping zone (at t = 0.24s). As a consequence, the transformer differential protection element might issue incorrect tripping signal in these cases.

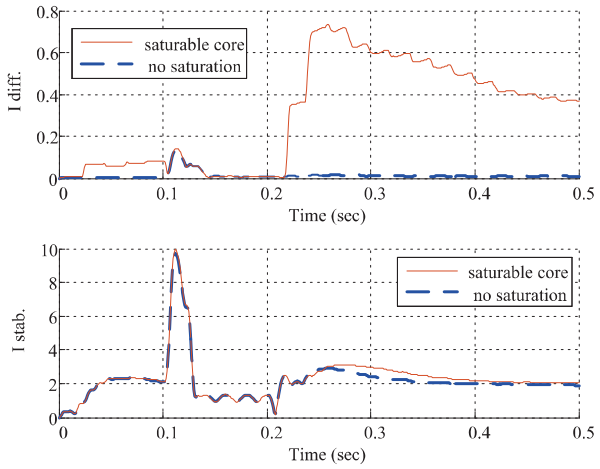

Figure 9Simulated differential and stabilizing currents with external 3-phase fault.

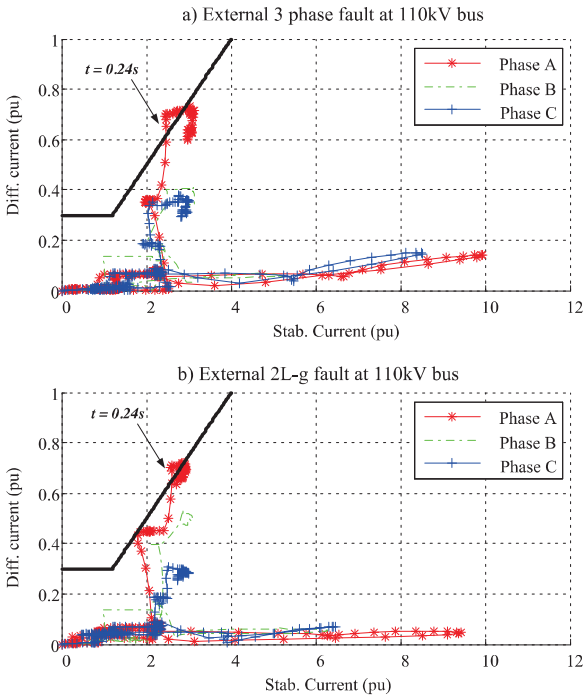

Figure 10 Transformer differential protection, with and without crowbar.

The performance of the differential protection when a 3-phase fault occurs at the 22kV bus is shown in Fig. 11. In this case, the differential relay operates correctly.

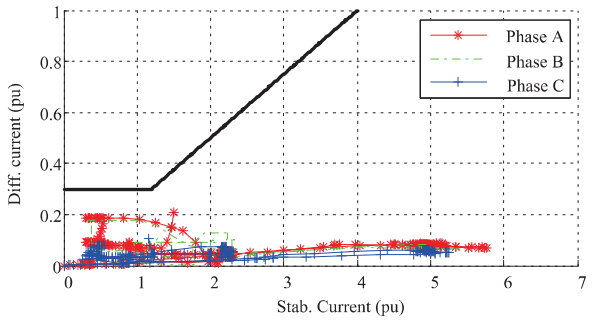

Figure 11 Transformer differential protection with 3-phase fault at 22kV bus.

C. *Second harmonic blocking*

From the simulation results in Fig. 10, one straight forward solution to avoid possible incorrect tripping is to enlarge the restraint area of the differential protection. However, in this study we also want to investigate the harmonic content of fault current and how it may affect the transformer differential protection. Fig. 12 show the second order harmonic, in percentage of the fundamental frequency, in case of a 2-phase-to-ground fault at 110kV bus, with crowbar activated, and transformer saturable core is considered. It can be seen that the second harmonic is very high after the moments of fault inception and fault clearing. There is a distinctive difference between 2nd harmonic content of differential currents in case of external and internal fault. In case of an internal fault, the 2nd harmonic content decays very quickly after 1-2 cycles. On the other hand, in case of the external fault, the 2nd harmonic current is fairly high, both during fault and during 2-3 cycles after fault clearing. This result suggests that the 2nd harmonic blocking logic in the transformer differential protection element might be used to prevent incorrect tripping in case of an external fault, and also to prevent incorrect tripping due to the fault clearing current.

V. CONCLUSION

The current paper investigates the performance of the transformer differential relaying scheme, when it is connected to a type III wind farm. The simulation model takes into account high order dynamics of the wind farm, as well as several controllers such as the crowbar protection and the current limiter circuit. The current transformers with saturation characteristic are also modeled.

The simulation results have shown that fault currents from the type III wind farm may cause mal-operation of the transformer differential protection. It should be noted that there are many factors that affect the fault current, as well as the differential relay performance: crowbar activation logic, crowbar resistance, control parameters for the grid-side and rotor-side converters, etc. In order to evaluate the performance of the protective relaying system with fault current from wind farm, more exhaustive simulation scenarios need to be considered. However, the simulation results from this work show that fault clearing current of DFIG wind farm might cause incorrect operation of the differential protection. This possible mal-operation might be mitigated by properly adjusting the 2nd harmonic blocking logic. Alternatively, the characteristic of differential protection might be changed (enlarged), to further ensure robustness of the differential protection element with regard to external faults.

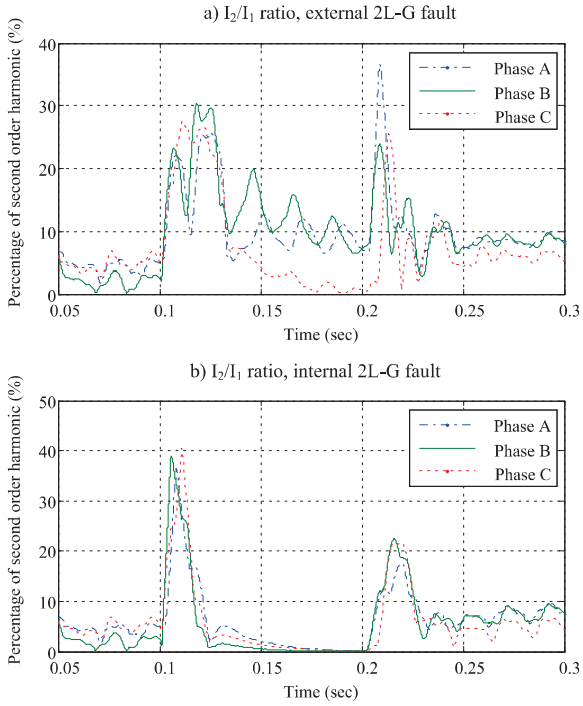

Figure 12Second harmonic (in percentage), with internal and external faults.

In our future work, the simulated fault currents will be converted to a COMTRADE data format [11], which can be used to test real digital relays, using appropriate relay test sets. The proposed framework can also be extended to analyze the effect of other inverter-based generation sources, such as solar generators and battery storage devices on the digital relaying performance.

ACKNOWLEDGEMENT

This work was supported by the Hanoi University of Science and Technology research fund T2015-152, along with the Hitachi Global Foundation award 2017.

REFERENCES

[1] J. B. et al, "Fault current contributions from wind plants," Electric Machinery Committee and Power System Relaying Committee of the IEEE PES, A report to the T&D Committee, 2012.

[2] NREL, "Short circuit current contribution for different wind turbine generator types," in *Power and Energy Society General Meeting*, 2010.

[3] R. Jain, B. Johnson, and H. Hess, "Performance of line protection and supervisory elements for doubly fed wind turbines," in *Power and Energy Society General Meeting*, 2015.

[4] B. Gao, W. Wei, L. Zhang, N. Chen, Y. Wu, and Y. Tang, "Differential protection for an outgoing transformer of large-scale doubly fed induction generator-based wind farms," *Energies*, vol. 7, no. 9, p. 5566, 2014. [Online]. Available: http://www.mdpi.com/1996-1073/7/9/5566

[5] G. Abad, J. Lpez, M. Rodriguez, L. Marroyo, and G. Iwanski, *Doubly Fed Induction Machine: Modeling and Control for Wind Energy Generation Applications*, W. Press, Ed., 2011.

[6] J. J. Sanchez-Gasca, W. Price, and R. Delmerico, "Dynamic modeling of GE 1.5 and 3.6 mw wind turbine-generators for stability simulations," in *Power and Energy Society General Meeting*, 2003.

[7] "IEEE guide for protecting power transformers," *IEEE Std C37.91-2008 (Revision of IEEE Std C37.91-2000)*, pp. 1–139, May 2008.

[8] IEEE Power Engineering Society. IEEE Power system Relaying Committee, "Theory for CT sat calculator,", Tech. Rep., 2003.

[9] SIEMENS, "SIPROTEC 7UT613/63x instruction manual," Tech. Rep.

[10] S. Patel, "Fundamentals of transformer inrush," in *64th Annual Conference for Protective Relay Engineers*, April 2011, pp. 290–300.

[11] IEEE Power Engineering Society. Power Systems Relaying Committee., Institute of Electrical and Electronics Engineers., and IEEE-SA Standards Board., *IEEE standard common format for transient data exchange (COMTRADE) for power systems*. Institute of Electrical and Electronics Engineers, 1999.